VOLUME 34 NUMBER 5

ACCOUNTS of CHEMICAL RESEARCH®

MAY 2001

The Reaction of Cl with CH_4: A Connection between Kinetics and Dynamics

HOPE A. MICHELSEN

Combustion Research Facility, Sandia National Laboratories, MS 9055, P.O. Box 969, Livermore, California 94551

Received August 9, 2000

ABSTRACT

This paper presents an analysis of the reaction of Cl with CH_4 by combining measurements of thermal rate constants and state-dependent reaction cross sections. State-dependent measurements have shown that the reaction probability is enhanced by vibrational excitation of CH_4. Measured thermal rate constants were fit with a model incorporating this information. The results provide estimates of rate constants at extreme temperatures and information about the temperature and collision energy dependence of the vibrational enhancement.

Introduction

The reaction of atomic chlorine with methane,

$$Cl + CH_4 \rightarrow CH_3 + HCl$$

is one of the few gas-phase reactions that control the partitioning of inorganic chlorine throughout the stratosphere.[1] This reaction plays a critical role in limiting stratospheric ozone loss via catalytic cycles involving chlorine radicals[2−5] and may similarly restrict ozone destruction while providing a significant sink for CH_4 in the marine boundary layer.[6,7] Differences between the rate constants of $Cl + {}^{12}CH_4$ and those of its isotopic analogues $Cl + {}^{13}CH_4$ (the carbon kinetic isotope effect) and $Cl + {}^{12}CH_3D$ (the hydrogen kinetic isotope effect) have caused this reaction to have a significant influence on the isotopic fractionation of tropospheric and stratospheric CO and CH_4.[8−14] This reaction has also been identified as the mechanism that initiates the production of higher molecular weight hydrocarbons and soot during the combustion of CH_4 in the presence of chlorinated species.[15−20] Recent work has shown that the deprotonation of CH_4 by Cl can be used to accelerate growth of diamond films by chemical vapor deposition.[21] The wide-ranging importance of $Cl + CH_4$ has prompted numerous kinetics studies,[22−36] largely for the purpose of providing rate constants for use in atmospheric and combustion models. Moreover, the relative simplicity of this six-atom system has inspired a number of experimental investigations[37−43] of the molecular dynamics and theoretical studies[24,26,31,44−56] of the dynamics and kinetics of this reaction.

The first part of this paper presents a brief review of what is known about $Cl + CH_4$ by qualitatively integrating information gained through molecular dynamics measurements with information derived from chemical kinetics measurements. An approach for more quantitatively combining internal-state-dependent measurements with thermal rate constant data is then presented. This approach demonstrates how the state-specific studies complement the thermal rate constant measurements and provides a means for integrating all available data into a more complete description of this reaction. The goal is to combine disparate data sets for practical applications without relying on the development of accurate potential energy surfaces or theoretical methodologies.

What Is Known about $Cl + CH_4$

The ground-state reaction of Cl with CH_4 is endothermic by ~600 cm^{-1} and activated by 840−1130 cm^{-1}.[23−31] Kinetics experiments[22−31] have yielded a pre-exponential factor of $\sim 1 \times 10^{-11}$ cm^3 $molecule^{-1}$ s^{-1}, which is ~30 times smaller than the hard-sphere collision rate at room temperature. Such a disparity between the pre-exponential factor and the hard-sphere collision rate is often indicative of tight steric restrictions on the reaction

Hope A. Michelsen was born in Portland, ME, in 1961. She received an A.B. in Chemistry from Dartmouth College (1984) and a Ph.D. in Chemistry with a minor in Physics from Stanford University (1993). She completed an NSF postdoctoral fellowship in Chemistry and Earth and Planetary Sciences at Harvard University in 1997, and is currently a Senior Member of the Technical Staff in the Combustion Research Facility at Sandia National Laboratories. Her research program includes studies of stratospheric chemistry and transport and the development of optical techniques for soot detection in diesel and gasoline engine exhaust.

10.1021/ar000066z CCC: $20.00
Published on Web 03/29/2001

geometry that must be accommodated in order for the reaction to proceed. Theoretical studies have shown that such restrictions apply to the ground-state reaction of Cl with CH_4 for which the transition state is tightly constrained to a collinear geometry.[45−47,49,51] A collinear transition state is supported by measurements demonstrating that the angular distribution of the HCl product is predominantly backscattered (with respect to the direction of approach of Cl),[38−40] the angular distribution for the CH_3 product is forward-scattered,[37] and the internal state distributions of the products are rotationally cold.[37−40]

Kinetics measurements yield an activation energy of ~900 cm^{-1} at temperatures below 300 K[23−31] and ~1100 cm^{-1} at higher temperatures,[22−26] demonstrating that this reaction cannot be represented by a simple Arrhenius expression (a single exponential dependence on inverse temperature). Non-Arrhenius behavior is commonly observed and can be attributed to a variety of factors. Heneghan et al.[24] showed that the curvature observed for the Cl + CH_4 reaction at high temperatures could be reproduced using the estimated temperature dependence of the transition-state heat capacity. A number of studies have indicated that tunneling contributes to the curvature in the Arrhenius plot (the semi-log plot of the rate constant vs inverse temperature) at low temperatures.[23,26,35,49,50,55,56] Ravishankara and Wine[32] alternatively hypothesized that differential reactivity of thermally accessible electronic states of Cl may be responsible for the non-Arrhenius behavior and the large variability in the low-temperature measurements. The electronic quenching rates on which their analysis was based have since been demonstrated to be inaccurate, however, and recent studies have indicated that the reaction of CH_4 with electronically excited Cl is not significantly faster than that with the ground state of Cl.[34,37,43] Kandel and Zare[37] suggested that the observed non-Arrhenius behavior could result from differential reactivity of low-frequency vibrational states of CH_4.

Simpson et al.[38,39] recently measured the relative state-dependent reaction cross sections and product angular and internal state distributions for the Cl + CH_4 reaction. By directly pumping the asymmetric CH stretch (ν_3) of CH_4 with an IR laser, they demonstrated that exciting one quantum of the stretch enhances the reaction probability by a factor of ~30 and leads to more forward- and side-scattered HCl product with more rotational energy than observed for the ground-state reaction. Simpson et al.[38,39,41] suggested that vibrational excitation of the CH stretch opens the cone of acceptance for reaction by relaxing the tight steric restrictions of the collinear transition state.

Kandel and Zare[37] extended the studies of the ground-state reaction to a wider range of collision energies. Instead of probing HCl, they probed the CH_3 produced by the reaction and observed products with more translational energy than could be accounted for by the energetics of the reaction. They noted that these energy discrepancies could be explained by reactions involving thermally populated excited states of the low-frequency bending modes of CH_4 if excitation of the umbrella (ν_4) and/or torsional (ν_2) modes of CH_4 also enhances reactivity of CH_4 with Cl. More side-scattered CH_3 product was observed from the reaction that they associated with CH_4 in one of these bending modes than for reaction with ground-state CH_4, and they speculated that the bending mode also relaxes the collinear requirement for the transition state.[37]

Earlier work by Hsu and Manuccia[57−59] indicated that pumping the CH_2 rocking mode (ν_7) of CH_2D_2 enhances the reaction rate with Cl. In contrast, Vijin et al.[60] noted no enhancement in reactivity when directly pumping the umbrella bending mode of CD_4 in a mixture of CH_4 and CD_4 and measuring the isotopic fractionation of products. Chesnokov et al.[61] pumped the asymmetric stretch of CH_4, which rapidly transfers energy to the bending modes at higher pressures, and similarly observed no enhancement in reactivity. Given their experimental uncertainties, they estimated that exciting the bending modes does not increase the reaction probability by more than a factor of 30−70 at 148 K, and exciting the stretching modes could increase the reaction probability by no more than a factor of 3000 at 173 K and 1200−1300 at 298 K.[61]

Theoretical investigations[49,52−54] employing variational transition state theory and multidimensional quantum scattering calculations support observations of vibrational enhancement. Theory[49,52] suggests, however, that exciting the symmetric stretch (ν_1) mode should be more effective at promoting the reaction than exciting the umbrella bend mode and that the asymmetric stretch and torsional bend modes do not couple strongly to the reaction coordinate and therefore should not be particularly effective. Using a model that combines information from dynamics and kinetics measurements, Michelsen and Simpson[35] showed that the non-Arrhenius behavior observed for this reaction at high temperatures could be explained exclusively by excitation of the stretching modes of CH_4. At low temperatures, the apparent curvature in the Arrhenius plot could be accounted for by tunneling and modest reaction rate enhancement by a low-frequency bending mode. The vibrational enhancement factors derived using this model are consistent with values reported by Simpson et al.[39] for the asymmetric stretch and with theoretical predictions for the symmetric stretch and umbrella bend. As shown below, however, this model cannot reconcile the thermal rate constant data with the hypothesis put forward by Kandel and Zare[37] that the bending modes enhance the reaction rate as much as, or more than, the stretching modes.

A Direct Connection between Kinetics and Dynamics

Total reaction cross sections and temperature-dependent thermal rate constants can be derived from state-dependent data for a reaction if the reaction probability has been measured in sufficient detail as a function of translational, vibrational, and rotational energy. This concept is straightforward and intuitive and has been discussed many times and in great detail over the past several decades.[62−70]

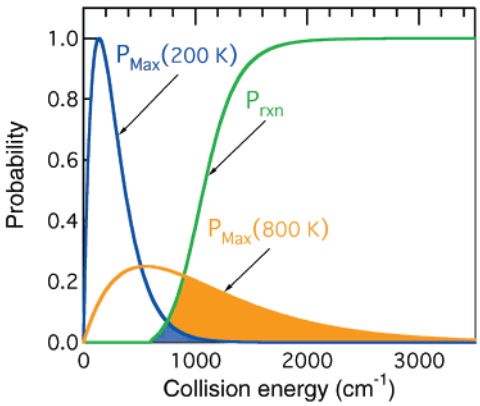

FIGURE 1. Energy dependence of the reaction probability. The reaction probability (green) is shown as a function of collision energy for a hypothetical reaction with an activation barrier of ~1150 cm^{-1}. The Maxwell speed distribution is shown for 200 K (blue) and 800 K (orange), and the shaded regions represent the overlap of the speed distribution with the reaction probability function for 200 K (blue shaded region) and 800 K (blue and orange shaded regions).

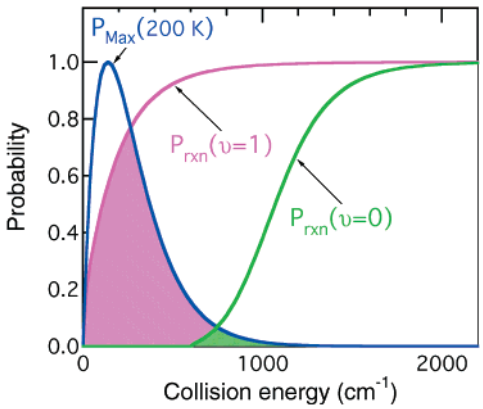

FIGURE 2. Energy dependence of the reaction probability for separate vibrational states. The reaction probability for the ground state (green) is shown as a function of collision energy for a hypothetical reaction with an activation barrier of ~1150 cm^{-1}. If the reaction probability of the excited vibrational state (magenta) is higher at lower collision energies, the reaction rate will be enhanced by vibration. The Maxwell speed distribution is shown for 200 K (blue), and the shaded regions represent the overlap of the speed distribution with the reaction probability functions for each vibrational state. For $\nu = 0$ the overlap is represented by the green shaded region, and for $\nu = 1$ the overlap is represented by the green and magenta shaded regions.

Derivations of the rate constant are based on "counting" the number of collisions that occur between molecules with sufficient energy to overcome the barrier. The probability of reaction per collision is determined by the overlap of the Maxwell speed distribution with the function defining the probability that the reaction will proceed at a particular collision energy $P_{rxn}(E_{coll})$. Ideally $P_{rxn}(E_{coll})$, often referred to as the "excitation function", has been measured at all collision energies, from well below to well above the reaction barrier. If all internal states react with the same probability, the rate constant is given by the overlap of $P_{rxn}(E_{coll})$ with the normalized Maxwell speed distribution $P_{Max}(E_{coll},T)$ expressed in terms of the collision energy E_{coll}. This integral over collision energy is then weighted by the collision frequency $Z(T)$ at temperature T, i.e.,

$$k(T) = Z(T) \int_0^\infty P_{rxn}(E_{coll}) P_{Max}(E_{coll},T)\, dE_{coll} \qquad (1)$$

As shown graphically in Figure 1 for a hypothetical reaction with an effective activation barrier of 1150 cm^{-1}, the overlap increases as the temperature increases, and more molecules have sufficient energy to react. For a real system, the maximum probability of reaction is not likely to be unity. At energies above the barrier height, the probability will be limited by factors such as steric effects and quantum mechanical reflection from the barrier.

The reaction probability for the Cl + CH_4 reaction has been shown to be sensitive to the vibrational state of CH_4. In this case, the rate constant for each vibrational state of CH_4 is calculated by replacing $P_{rxn}(E_{coll})$ with a vibrational-state-dependent function $P_{rxn}(E_{coll},\nu_i)$ in eq 1 and proceeding with the integration, as shown graphically in Figure 2. Each state makes a distinct contribution to the rate constant. The total rate constant is thus given by the sum of these contributions, each weighted by the population in that state, i.e.,

$$k(T) = Z(T) \sum_i S_i(T) \int_0^\infty P_{rxn}(E_{coll},\nu_i) P_{Max}(E_{coll},T)\, dE_{coll} \qquad (2)$$

where $S_i(T)$ is the Boltzmann factor for the population of reactant molecules in vibrational state ν_i. One can also imagine a reaction that depends on the rotational or electronic state of the reactant, in which case the summation in eq 2 would include terms corresponding to reactions involving these states. Because the rotational state dependence of the Cl + CH_4 reaction is not known, and the reaction appears to be insensitive to the electronic state of Cl,[34,37,43] only the vibrational state dependence of the reaction probability is considered here.

Despite such simplifying assumptions, a further complication prevents the calculation of thermal rate constants for Cl + CH_4 (or most other activated gas-phase reactions) directly from state-dependent measurements: state-dependent measurements are unavailable at enough collision energies to determine $P_{rxn}(E_{coll},\nu_i)$. The barrier estimated for the Cl + CH_4 reaction is low (1200−1700 cm^{-1}),[45−55] and state-dependent cross-section measurements are available only at selected collision energies (1050−2280 cm^{-1}) close to the barrier height and above,[37−39] whereas the Maxwell speed distribution is centered at collision energies well below the reaction barrier. State-dependent measurements at collision energies that are low enough to allow such an analysis are rare. Molecular beam experiments and measurements of $P_{rxn}(E_{coll})$ initiated by photolytic production of a reactant are often restricted to collision energies close to or above the barrier height. Nevertheless, such an analysis has been performed for several gas-phase activated[64,65] and barrierless[66−69] reactions based on molecular beam measurements of $P_{rxn}(E_{coll},\nu_i)$. Thermal rate constants have also been derived

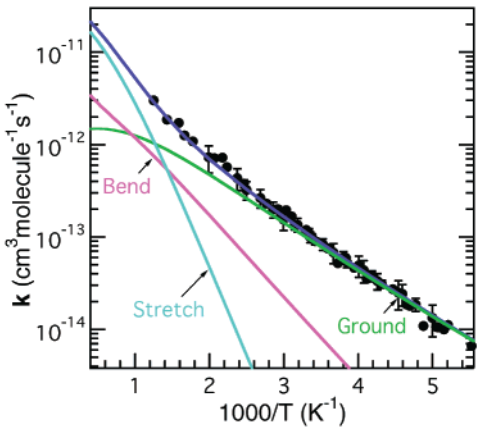

FIGURE 3. Arrhenius (semilogarithmic) plot of measured and calculated rate constants for $Cl + CH_4 \rightarrow CH_3 + HCl$. A weighted average of rate constants is shown as a function of inverse temperature (black circles) with 2σ error bars.[35] The purple line represents the result of a fit to the data using the model described in the text.[35] The other lines demonstrate the contribution to the rate constant from the stretching mode (cyan), the bending mode (magenta), and the vibrational ground state (green).

for one activated gas−surface reaction for which the reaction probability function depends on vibrational and rotational state.[70,71]

Although all of the necessary information may not be available to derive thermal rate constants directly from state-dependent measurements for $Cl + CH_4$, the approach described above can be used as a tool for the analysis of disparate data sets. By assuming a realistic functional form for $P_{rxn}(E_{coll},\nu_i)$, eq 2 can be fit to available thermal rate constant data. The results of such a fit can provide additional information about the energetics of the reaction. Moreover, this approach allows even limited information from state-dependent reaction cross-section measurements to be applied to the analysis of kinetics experiments. Similar fits to thermal rate data for this and other reactions have been successfully performed using functions derived from transition state theory to test kinetic and thermodynamic data and theoretical assumptions.[56,72,73]

Dynamics → Kinetics: Vibrational Enhancement and Non-Arrhenius Behavior

Assuming that both the stretching and bending modes of CH_4 enhance the reaction probability for $Cl + CH_4$,[37−39,57−59] the description of the rate constant by eq 2 must contain at least three terms, each of which is characterized by a distinct $P_{rxn}(E_{coll},\nu_i)$. Figure 3 shows a fit of eq 2 to the absolute rate constants measured for $Cl + CH_4$, with one term representing the nearly isoenergetic symmetric and asymmetric stretching modes, one term representing the umbrella bend mode, and one term representing the ground-state and torsional mode, which was assumed not to couple strongly to the reaction coordinate.[35] The functional form used to represent $P_{rxn}(E_{coll},\nu_i)$ for each state was given by the transmission coefficient estimated for tunneling through an unsymmetrical Eckart barrier, i.e., the function shown in Figure 1.[35] The contribution from

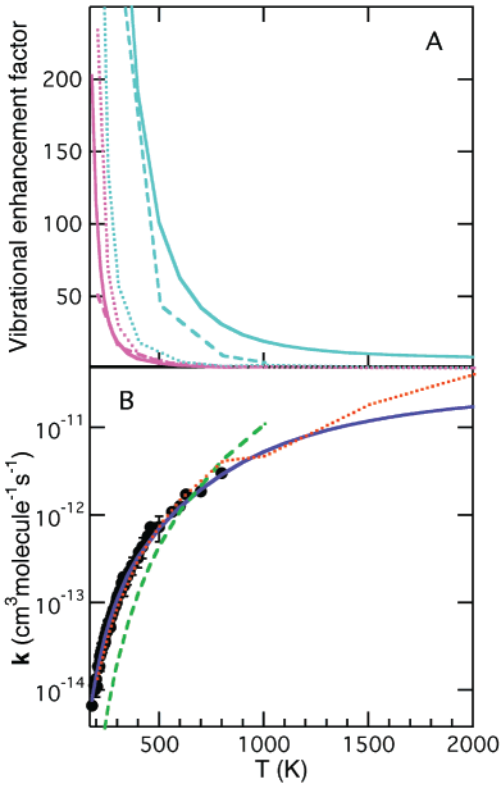

FIGURE 4. Temperature dependence of vibrational enhancement factors and rate constant predictions. (A) Vibrational enhancement (relative to thermal rate constants) is shown as a function of temperature for the bending (magenta) and stretching (cyan) modes. The results of the model described in the text[35] (solid) are compared with results of variational transition state calculations from Duncan and Truong[49] (dashed) and Corchado et al.[52] (dotted). (B) The average rate constants shown in Figure 3 are plotted with 2σ error bars as a function of temperature. Lines represent results from the model described in the text[35] (solid), Duncan and Truong[49] (dashed), and Corchado et al.[52] (dotted).

each of these terms is also shown. The results suggest that, at temperatures above ~600 K, the rate constant is dominated by reactions involving the excited stretching mode, whereas the low-temperature rate constant is predominantly determined by ground-state reactions. Thus, the curvature in the Arrhenius plot at high temperatures is attributable to the enhancement in the reaction probability by the excited stretching modes and the increase in the population of these excited modes with increasing temperature. The model results indicate that an increase in the tunneling probability for the ground-state reaction with decreasing temperature is responsible for curvature in the Arrhenius plot at low temperature. This low-temperature curvature may also be partially attributable to enhancement of the reaction probability by the umbrella bending mode, which has a significantly lower vibrational frequency than the stretching modes and thus higher populations at lower temperatures. Such curvature reduces the activation energy and pre-exponential factor inferred from fits to rate constant data for these temperatures.

Michelsen and Simpson[35] used these results to extrapolate the thermal rate constant data to temperatures above

800 K for which measurements are not available. They also used these results to reduce uncertainty in the thermal rate constant at temperatures below 260 K for which available measurements are inconsistent.[74,75] Because the model is based on a physical description of the reaction, Michelsen and Simpson[35] argued that these results are more reliable than simple fits to the data using an Arrhenius expression.

Kinetics → Dynamics: Relative Vibrational Enhancement by Bend and Stretch

Using the results of the fit to the thermal rate constant data, one can determine how much the bending and stretching modes enhance the reaction probability. Figure 4a shows the enhancement of the reactivity by these modes relative to thermal rate constants, i.e., the rate constant for each state (not weighted by the Boltzmann factor) divided by the total rate constant. As temperature decreases, the enhancement factors increase, although the overall rate constant decreases. Results are shown both for the model described here and for variational transition state theory calculations by Duncan and Truong[49] and Corchado et al.[52] Predictions from all three studies suggest that the stretching modes should enhance the reactivity by more than the bending mode, although the results of Corchado et al.[52] indicate that the difference between the stretch and bend is not as large as implied by the other two studies. Figure 4b shows the corresponding predictions of the thermal rate constants compared with experimental values. The potential energy surface (PES) used by Corchado et al.[52] was adjusted to give good agreement with room-temperature rate constant measurements and thus yields good agreement with experimental data and with the model described above, which was fit to the data. At higher temperatures the predictions deviate from one another. Confidence in the accuracy of the PES developed by Corchado et al.[52] is diminished, however, by the lack of agreement between predictions based on this PES and experimental measurements of the carbon and hydrogen kinetic isotope effects.[36]

Recent experimental results suggest that the bending mode should be at least as effective as, if not more effective than, the stretch at promoting the reaction. Figure 5 shows the measured[41−43] and modeled vibrational enhancement by these modes relative to the ground-state reaction probability. Calculated values were determined as a function of collision energy for an estimated experimental energy distribution.[76] The model is in good agreement with the work of Simpson et al.[38,39] but in poor agreement with the measurements of Kandel and Zare.[37] Whereas the results of Simpson et al.[38,39] were obtained by directly pumping the asymmetric stretching mode and comparing the results with the ground-state reaction, the experimental results of Kandel and Zare[37] were based on conjecture that excess translational energy observed in the products could be attributable to reagent vibrational energy from thermally populated bending modes of CH_4. Although an alternative explanation for excessively fast products is not obvious, the present interpretation is inconsistent with the thermal rate constant measurements within the context of this model.

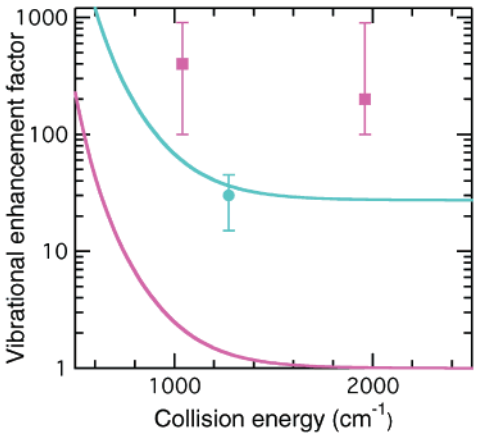

FIGURE 5. Energy dependence of vibrational enhancement factors. Enhancement of the reaction probability for the bending (magenta) and stretching (cyan) modes relative to the reaction probability of the ground state is shown as a function of the collision energy. The results of the present study (lines) is compared with results of state-dependent cross-section measurements from Simpson et al.[38,39] for the asymmetric stretch (circle) and Kandel and Zare[37] for the bend (squares). The error bars represent $\pm 2\sigma$ uncertainty for the stretch and are approximate estimates for the bend (S. A. Kandel, private communication, 2000).

Conclusions

The present analysis demonstrates that results from kinetics and dynamics experiments can, under some conditions, be combined to provide a more complete description of a reaction. The additional information derived from such an analysis may be useful for resolving outstanding uncertainties or discrepancies in the interpretation of experimental results. For the Cl + CH_4 reaction, the results of dynamics experiments have been included in a model, which was fit to thermal rate constant data.

Of course, there are a great number of significant uncertainties associated with this approach. In the work reviewed here, potentially important factors, such as the possible influence of CH_4 rotational states on the reactivity, were neglected. In addition, a functional form for the collision energy dependence of the reaction probability was based on a simplified mechanism for tunneling, which does not account for multidimensional tunneling contributions. Previous work has suggested, however, that neglecting multidimensional tunneling effects is not a serious oversight for this reaction.[72] This method also requires thermal rate data recorded with good precision over a reasonably large temperature range. Despite these limitations, this technique can be used to consolidate information from kinetics and dynamics experiments for selected reactions.

As shown here, such an approach can be used to extrapolate rate constant measurements to temperatures where data are currently unavailable and to reduce uncertainties where current measurements are inconsistent. The fit of this model to thermal rate constant

measurements has, in turn, provided information about the relative importance of stretching and bending modes in the vibrational enhancement of the reaction rate. As with many experimental and theoretical studies, this analysis has provided new questions that can be resolved only with additional experimental and theoretical work.

I thank R. L. Farrow, D. M. Golden, S. A. Kandel, D. A. V. Kliner, S. J. Klippenstein, K. T. Lorenz, A. McIlroy, D. L. Osborn, W. R. Simpson, and C. A. Taatjes for enlightening discussions and helpful suggestions. This work was supported by the Division of Chemical Sciences, Geosciences, and Biosciences, the Office of Basic Energy Sciences, the U.S. Department of Energy, and the National Aeronautics and Space Administration, Atmospheric Chemistry Modeling and Analysis Program.

References

(1) Solomon, S. Stratospheric Ozone Depletion: A Review of Concepts and History. *Rev. Geophys.* **1999**, *37*, 275−316 and references therein.
(2) Prather, M.; Jaffe, A. H. Global Impact of the Antarctic Ozone Hole: Chemical Propagation. *J. Geophys. Res.* **1990**, *95*, 3473−3492.
(3) Douglass, A. R.; et al. Interhemispheric Differences in Springtime Production of HCl and $ClONO_2$ in the Polar Vortices. *J. Geophys. Res.* **1995**, *100*, 13967−13978.
(4) Santee, M. L.; et al. Chlorine Deactivation in the Lower Stratospheric Polar Regions during Late Winter: Results from UARS. *J. Geophys. Res.* **1996**, *101*, 18835−18859.
(5) Michelsen, H. A.; et al. Maintenance of High HCl/Cl_y and NO_x/NO_y in the Antarctic Vortex: A Chemical Signature of Confinement during Spring. *J. Geophys. Res.* **1999**, *104*, 26419−26436.
(6) Oum, K. W.; Lakin, M. J.; DeHaan, D. O.; Brauers, T.; Finlayson-Pitts, B. J. Formation of Molecular Chlorine from Photolysis of Ozone and Aqueous Sea-Salt Particles. *Science* **1998**, *279*, 74−77.
(7) Keene, W. C.; Jacob, D. J.; Fan, S.-M. Reactive Chlorine: A Potential Sink for Dimethylsulfide and Hydrocarbons in the Marine Boundary Layer. *Atmos. Environ.* **1996**, *30*, i−iii.
(8) Brenninkmeijer, C. A. M.; et al. A Large ^{13}CO Deficit in the Lower Antarctic Stratosphere due to "Ozone Hole" Chemistry: Part I, Observations. *Geophys. Res. Lett.* **1996**, *23*, 2125−2128.
(9) Müller, R.; Brenninkmeijer, C. A. M.; Crutzen, P. J. A Large ^{13}CO Deficit in the Lower Antarctic Stratosphere due to "Ozone Hole" Chemistry: Part II, Modeling. *Geophys. Res. Lett.* **1996**, *23*, 2129−2132.
(10) Gupta, M.; Tyler, S.; Cicerone, R. Modeling Atmospheric $\delta^{13}CH_4$ and the Causes of Recent Changes in Atmospheric CH_4 Amounts. *J. Geophys. Res.* **1996**, *101*, 22923−22932.
(11) Tyler, S. C.; et al. Stable Carbon Isotope Composition of Atmospheric Methane: A Comparison of Surface Level and Free Tropospheric Air. *J. Geophys. Res.* **1999**, *104*, 13895−13910.
(12) Bergamaschi, P.; et al. Implications of the Large Carbon Kinetic Isotope Effect in the Reaction CH_4 + Cl for the $^{13}C/^{12}C$ Ratio of Stratospheric CH_4. *Geophys. Res. Lett.* **1996**, *23*, 2227−2230.
(13) Sugawara, S.; et al. Vertical Profile of the Carbon Isotopic Ratio of Stratospheric Methane over Japan. *Geophys. Res. Lett.* **1997**, *24*, 2989−2992.
(14) Irion, F. W.; et al. Stratospheric Observations of CH_3D and HDO from ATMOS Infrared Solar Spectra: Enrichments of Deuterium in Methane and Implications for HD. *Geophys. Res. Lett.* **1996**, *23*, 2381−2384.
(15) Le Bec, R.; Marquaire, P.-M.; Côme, G.-M. Formation of C_{2+} Hydrocarbons in CH_4/O_2 Diffusion Flames with Cl, CH_3Cl, and HCl Additives. *Ind. Eng. Chem. Res.* **1990**, *29*, 539−544.
(16) Senkan, S. M.; Robinson, J. M.; Gupta, A. K. Sooting Limits of Chlorinated Hydrocarbon-Methane-Air Premixed Flames. *Combust. Flame* **1983**, *49*, 305−314.
(17) Weissman, M.; Benson, S. W. Pyrolysis of Methyl Chloride, a Pathway in the Chlorine-Catalyzed Polymerization of Methane. *Int. J. Chem. Kinet.* **1984**, *16*, 307−333.
(18) Frenklach, M. Production of Polycyclic Aromatic Hydrocarbons in Chlorine Containing Environments. *Combust. Sci. Technol.* **1990**, *74*, 283−296.
(19) Venkatesh, S.; Saito, K. Estimates on the Effect of Chlorine on the Global Soot Production Rates in Laminar Hydrocarbon-Air Diffusion Flames. *Combust. Sci. Technol.* **1992**, *85*, 297−311.
(20) Mitchell, T. J.; Benson, S. W.; Karra, S. B. Kinetic Model for Formation of Aromatics in the High-Temperature Chlorination of Methane. *Combust. Sci. Technol.* **1995**, *107*, 223−260.
(21) Wu, J.-J.; Hong, C.-N. Effect of Chlorine Addition on Diamond Growth using Methane/Hydrogen Reactants. *J. Appl. Phys.* **1997**, *81*, 3647−3651.
(22) Pritchard, H. O.; Pyke, J. B.; Trotman-Dickenson, A. F. The Study of Chlorine Atom Reactions in the Gas Phase. *J. Am. Chem. Soc.* **1955**, *77*, 2629−2633.
(23) Whytock, D. A.; Lee, J. H.; Michael, J. V.; Payne, W. A.; Stief, L. J. Absolute Rate of the Reaction of $Cl(^2P)$ with Methane from 200−500 K. *J. Chem. Phys.* **1977**, *66*, 2690−2695.
(24) Heneghan, S. P.; Knoot, P. A.; Benson, S. W. The Temperature Coefficient of the Rates in the System Cl + $CH_4 \rightleftarrows CH_3$ + HCl, Thermochemistry of the Methyl Radical. *Int. J. Chem. Kinet.* **1981**, *13*, 677.
(25) Keyser, L. F. Absolute Rate and Temperature Dependence of the Reaction between Chlorine (^2P) Atoms and Methane. *J. Chem. Phys.* **1978**, *69*, 214−218.
(26) Zahniser, M. S.; Berquist, B. M.; Kaufman, F. Kinetics of the Reaction Cl + $CH_4 \rightarrow CH_3$ + HCl from 200° to 500° K. *Int. J. Chem. Kinet.* **1978**, *X*, 15−29.
(27) Seeley, J. V.; Jayne, J. T.; Molina, M. J. Kinetic Studies of Chlorine Atom Reactions Using the Turbulent Flow Tube Technique. *J. Phys. Chem.* **1996**, *100*, 4019−4025.
(28) Wang, J. J.; Keyser, L. F. Kinetics of the $Cl(^2P_J)$ + CH_4 Reaction: Effects of Secondary Chemistry below 300 K. *J. Phys. Chem. A* **1999**, *103*, 7460−7469.
(29) Watson, R.; Machado, G.; Fischer, S.; Davis, D. D. A Temperature Dependence Kinetics Study of the Reactions of $Cl(^2P_{3/2})$ with O_3, CH_4, and H_2O_2. *J. Chem. Phys.* **1976**, *65*, 2126−2138.
(30) Manning, R. G.; Kurylo, M. J. Flash Photolysis Resonance Fluorescence Investigation of the Temperature Dependencies of the Reactions of $Cl(^2P)$ Atoms with CH_4, CH_3Cl, CH_3F, CH_3F†, and C_2H_6. *J. Phys. Chem.* **1977**, *81*, 291−296.
(31) Lin, C. L.; Leu, M. T.; DeMore, W. B. Rate Constant for the Reaction of Atomic Chlorine with Methane. *J. Phys. Chem.* **1978**, *82*, 1772−1777.
(32) Ravishankara, A. R.; Wine, P. H. A Laser Flash Photolysis-Resonance Fluorescence Kinetics Study of the Reaction $Cl(^2P)$ + $CH_4 \rightarrow CH_3$ + HCl. *J. Chem. Phys.* **1980**, *72*, 25−30.
(33) Pilgrim, J. S.; McIlroy, A.; Taatjes, C. A. Kinetics of Cl Atom Reactions with Methane, Ethane, and Propane from 292 to 800 K. *J. Phys. Chem. A* **1997**, *101*, 1873−1880.
(34) Matsumi, Y.; Izumi, K.; Skorokhodov, V.; Kawasaki, M.; Tanaka, N. Reactions and Quenching of $Cl(^2P_j)$ Atoms in Collisions with Methane and Deuterated Methanes. *J. Phys. Chem. A* **1997**, *101*, 1216−1221.
(35) Michelsen, H. A.; Simpson, W. R. Relating State-Dependent Cross Sections to Non-Arrhenius Behavior for the Cl + CH_4 Reaction. *J. Phys. Chem. A* **2001**, *105*, 1476−1488 and references therein.
(36) Michelsen H. A. Carbon and Hydrogen Kinetic Isotope Effects for the Reaction of Cl with CH_4: Consolidating Chemical Kinetics and Molecular Dynamics Measurements. *J. Geophys. Res.* **2001**, in press, and references therein.
(37) Kandel, S. A.; Zare, R. N. Reaction Dynamics of Atomic Chlorine with Methane: Importance of Methane Bending and Torsional Excitation in Controlling Reactivity. *J. Chem. Phys.* **1998**, *109*, 9719−9727.
(38) Simpson, W. R.; Rakitzis, T. P.; Kandel, S. A.; Orr-Ewing, A. J.; Zare, R. N. Reaction of Cl with Vibrationally Excited CH_4 and CHD_3: State-to-State Differential Cross Sections and Steric Effects for the HCl Product. *J. Chem. Phys.* **1995**, *103*, 7313−7335.
(39) Simpson, W. R.; Rakitzis, T. P.; Kandel, S. A.; Lev-On, T.; Zare, R. N. Picturing the Transition-State Region and Understanding Vibrational Enhancement for the Cl + $CH_4 \rightarrow$ HCl + CH_3 Reaction. *J. Phys. Chem.* **1996**, *100*, 7938−7947.
(40) Varley, D. F.; Dagdigian, P. J. Product State Distributions and Angular Differential Cross Sections from Photoinitiated Reactions of Chlorine Atoms with Small Hydrocarbons. *J. Phys. Chem.* **1995**, *99*, 9843−9853.
(41) Orr-Ewing, A. J.; Simpson, W. R.; Rakitzis, T. P.; Kandel, S. A.; Zare, R. N. Scattering-angle Resolved Product Rotational Alignment for the Reaction of Cl with Vibrationally Excited Methane. *J. Chem. Phys.* **1997**, *106*, 5961−5971.
(42) Aquilanti, V.; Cappelletti, D.; Pirani, F. Magnetically Selected Beams of Atomic Chlorine: Measurement of Long-range Features of the Chlorine−Hydrogen and Chlorine-Methane Potential-energy Surfaces. *J. Chem. Soc., Faraday Trans.* **1993**, *89*, 1467−1474.
(43) Tyndall, G. S.; Orlando, J. J.; Kegley-Owen, C. S. Rate Coefficients for Quenching of $Cl(^2P_{1/2})$ by Various Atmospheric Gases. *J. Chem. Soc., Faraday Trans.* **1995**, *91*, 3055−3061.

(44) Johnston, H. S.; Goldfinger, P. Theoretical Interpretation of Reactions Occurring in Photochlorination. *J. Chem. Phys.* **1962**, *37*, 700−709.
(45) Truong, T. N.; Truhlar, D. G.; Baldridge, K. K.; Gordon, M. S.; Steckler, R. Transition State Structure, Barrier Height, and Vibrational Frequencies for the Reaction Cl + CH_4 → CH_3 + HCl. *J. Chem. Phys.* **1989**, *90*, 7137−7142.
(46) Gonzalez-Lafont, A.; Truong, T. N.; Truhlar, D. G. Interpolated Variational Transition-State Theory: Practical Methods for Estimating Variational Transition-State Properties and Tunneling Contributions to Chemical Reaction Rates from Electronic Structure Calculations. *J. Chem. Phys.* **1991**, *95*, 8875−8894.
(47) Dobbs, K. D.; Dixon, D. A. Ab Initio Predition of the Activation Energy for the Abstraction of a Hydrogen Atom from Methane by Chlorine Atom. *J. Phys. Chem.* **1994**, *98*, 12584−12589.
(48) Wang, X.; Ben-Nun, M.; Levine, R. D. Peripheral Dynamics of the Cl + CH_4 → HCl + CH_3 Reaction. A Classical Trajectory Computation. *Chem. Phys.* **1995**, *197*, 1−17.
(49) Duncan, W. T.; Truong, T. N. Thermal and Vibrational-State Selected Rates of the Cl + CH_4 ↔ HCl + CH_3 Reaction. *J. Chem. Phys.* **1995**, *103*, 9642−9652.
(50) Espinosa-García, J.; Corchado, J. C. Analytical Potential Energy Surface for the CH_4 + Cl → CH_3 + ClH Reaction: Application of the Variational Transition State Theory and Analysis of the Kinetic Isotope Effects. *J. Chem. Phys.* **1996**, *105*, 3517−3523.
(51) Roberto-Neto, O.; Coitiño, E. L.; Truhlar, D. G. Dual-Level Direct Dynamics Calculations of Deuterium and Carbon-13 Kinetic Isotope Effects for the Reaction Cl + CH_4. *J. Phys. Chem. A* **1998**, *102*, 4568−4578.
(52) Corchado, J. C.; Truhlar, D. G.; Espinosa-García, J. Potential Energy Surface, Thermal, and State-Selected Rate Coefficients and Kinetic Isotope Effects for Cl + CH_4 → HCl + CH_3. *J. Chem. Phys.* **2000**, *112*, 9375−9389.
(53) Nyman, G.; Yu, H.-G.; Walker, R. B. Reduced Dimensionality Quantum Scattering Calculations on the Cl + CH_4 → HCl + CH_3 Reaction. *J. Chem. Phys.* **1998**, *109*, 5896−5904.
(54) Yu, H.-G.; Nyman, G. Three-Dimensional Quantum Scattering Calculations on the Cl + CH_4 ⇄ HCl + CH_3 Reaction. *Phys. Chem. Chem. Phys.* **1999**, *1*, 1181−1190.
(55) Yu, H.-G.; Nyman, G. A Four Dimensional Quantum Scattering Study of the Cl + CH_4 ⇄ HCl + CH_3 Reaction via Spectral Transform Iteration. *J. Chem. Phys.* **1999**, *110*, 7233−7244.
(56) Donahue, N. M. Revisiting the Hammond Postulate: The Role of Reactant and Product Ionic States in Regulating Barrier Heights, Locations, and Transition State Frequencies. *J. Phys. Chem. A* **2001**, *105*, 1489−1497.
(57) Hsu, D. S. Y.; Manuccia, T. J. Deuterium Enrichment by CW CO_2 Laser Induced Vibrational Photochemistry. In *Advances in Laser Chemistry*; Zewail, A. H., Ed.; Springer-Verlag: Berlin, 1978; pp 89−92.
(58) Hsu, D. S. Y.; Manuccia, T. J. Deuterium Enrichment by CW CO_2 Laser-induced Reaction of Methane. *Appl. Phys. Lett.* **1978**, *33*, 915−917.
(59) Manuccia, T. J.; Hsu, D. S. Y. Deuterium Enrichment by CW Vibrational Photochemistry of Methane-Economic Considerations. In *Laser-Induced Processes in Molecules*; Kompa, K. L., Smith, S. D., Eds.; Springer: Heidelberg, 1979; pp 270−271.
(60) Vijin, V. V.; Mikheev, A. N.; Petrov, A. K.; Molin, Y. N. Study of the Chlorination of CH_4 and CD_4 in a CO Laser Beam. *React. Kinet. Catal. Lett.* **1975**, *3*, 79−82.
(61) Chesnokov, E. N.; Strunin, V. P.; Serdyuk, N. K.; Panfilov, V. N. Reactivity of Vibrationally Excited Methane Molecules in Reactions with Chlorine Atoms. *React. Kinet. Catal. Lett.* **1975**, *3*, 131−137.
(62) Eliason, M. A.; Hirschfelder, J. O. General Collision Theory Treatment for the Rate of Bimolecular, Gas-Phase Reactions. *J. Chem. Phys.* **1959**, *30*, 1426−1436.
(63) Greene, E. F.; Kupperman, A. Chemical Reaction Cross Sections and Rate Constants. *J. Chem. Educ.* **1968**, *45*, 361−369.
(64) Che, D.-C.; Liu, K. Reactive Scattering of CN + D_2: The Stereodynamics. *Chem. Phys.* **1996**, *207*, 367−378.
(65) Hsu, Y.-T.; Wang, J.-H.; Liu, K. Reaction Dynamics of $O(^1D)$ + H_2, D_2, and HD: Direct Evidence for the Elusive Abstraction Pathway and the Estimation of its Branching. *J. Chem. Phys.* **1997**, *107*, 2351−2356.
(66) Mcdonald, R. G.; Liu, K.; Sonnenfroh, D. M.; Liu, D.-J. Crossed-beam Studies of Radical Reaction Dynamics: CN + O_2 → $NCO(\tilde{X}^2\Pi)$ + O. *Can. J. Chem.* **1994**, *72*, 660−673.
(67) Naulin, C.; Costes, M. Excitation Function of the Al + O_2 → AlO + O Reaction: A Comparison with Kinetics. *J. Phys. Chem.* **1994**, *98*, 5593−5596.
(68) Naulin, C.; Costes, M. Crossed-Beam Study of the $Al(^2P_{1/2,3/2})$ + $O_2(X^3\Sigma_g^-)$ → $AlO(X^3\Sigma^+)$ + $O(^3P_J)$ Reaction at Low and Very Low Kinetic Energies. *Chem. Phys. Lett.* **1999**, *310*, 231−239.
(69) Geppert, W. D.; et al. Comparison of the Cross-Sections and Thermal Rate Constants for the Reactions of $C(^3P_J)$ Atoms with O_2 and NO. *Phys. Chem. Chem. Phys.* **2000**, *2*, 2873−2881.
(70) Rettner, C. T.; Michelsen, H. A.; Auerbach, D. J. From Quantum-State-Specific Dynamics to Reaction Rates: The Dominant Role of Translational Energy in Promoting the Dissociation of D_2 on Cu(111) under Equilibrium Conditions. *Faraday Discuss.* **1993**, *96*, 17−31.
(71) Rettner, C. T.; Michelsen, H. A.; Auerbach, D. J. Quantum-State-Specific Dynamics of the Dissociative Adsorption and Associative Desorption of H_2 at a Cu(111) Surface. *J. Chem. Phys.* **1995**, *102*, 4625−4641.
(72) Furue, H.; Pacey, P. D. Properties of Activation Barriers from Thermal Rate Data on Forward and Reverse Reactions: OH + H_2, NH_2 + H_2, CH_3 + H_2, and CH_3 + HCl. *J. Chem. Phys.* **1990**, *94*, 1419−1425.
(73) Furue, H.; Pacey, P. D. Properties of Activation Barriers from Curved Arrhenius Plots: X + H_2 → XH + H. *J. Phys. Chem.* **1987**, *91*, 1584−1590.
(74) Sander, S. P.; et al. *Chemical Kinetics and Photochemical Data for Use in Stratospheric Modeling*; JPL Publication 00-3; Jet Propulsion Laboratory: Pasadena, CA, 2000.
(75) Atkinson, R.; et al. Evaluated kinetic and photochemical data for atmospheric chemistry, organic species: Supplement VII. IUPAC subcommittee on gas kinetic data evaluation for atmospheric chemistry. *J. Phys. Chem. Ref. Data* **1999**, *28*, 191−394.
(76) van der Zande, W. J.; Zhang, R.; Zare, R. N.; McKendrick, K. G.; Valentini, J. J. Superthermal widths of the collision energy distributions in hot atom reactions. *J. Phys. Chem.* **1991**, *95*, 8205−8207.

AR000066Z